Materials Science and Engineering B 324 (2026) 118907

Contents lists available at ScienceDirect

Materials Science & Engineering B

journal homepage: www.elsevier.com/locate/mseb

Enhanced O-phenylenediamine-doped PVDF/LiI/I_2 polymer electrolytes for dye-sensitized solar cells in adaptive portable assistive power device applications

K. Sathya [a], D. Janet [a], S. Kannadhasan [b], P. Sudhakar [c], S. Kotteswaran [a,*], Saravanan Pandiaraj [d,e], G Ahilandeswari [f], Gautham Devendrapandi [g], Ranjith Balu [h,*]

[a] Department of Chemistry, School of Basic Sciences, Vels Institute of Science Technology & Advanced Studies (VISTAS), Pallavaram, Chennai, 600117, India
[b] Sri Venkateswara College of Engineering and Technology, Thirupachur-631203, Tiruvallur, Tamil Nadu. India
[c] College of Chemical and Biological Engineering, Shandong University of Science and Technology, Qingdao 266590, China
[d] Department of Self-Development Skills, King Saud University, Riyadh, Saudi Arabia
[e] King Salman Center for Disability Research, 11614 Riyadh, Saudi Arabia
[f] Department of Physics, Rajalakshmi Engineering College, Chennai, Tamil Nadu, 602105, India
[g] Department of Computational Biology, Institute of Bioinformatics, Saveetha School of Engineering, Saveetha Institute of Medical and Technical Science, Thandalam, Chennai, Tamil Nadu, 602105, India
[h] Division of Research and Development Cell, Lovely Professional University, Phagwara, Punjab, 144411, India

ARTICLE INFO

Keywords:
O-Phenylenediamine
Polymer electrolyte
Dye sensitized solar cell
Polyvinylidene fluoride

ABSTRACT

Dye-sensitized solar cells (DSSCs) represent a promising solution to global energy demands owing to their cost-effectiveness, facile fabrication, and compatibility with sustainable materials. In this study, we investigate the impact of *o*-phenylenediamine doping on the structural and electrochemical properties of PVDF/LiI/I_2-based polymer electrolytes and the corresponding photovoltaic performance in DSSCs. A series of doped polymer electrolytes were synthesized via solution casting using *N*, *N*-dimethylformamide (DMF) as the solvent, with *o*-phenylenediamine incorporated at varying weight percentages (0–50 wt%). The structural modifications were characterized by SEM and XRD, revealing a significant reduction in crystallinity and the formation of uniformly dispersed, spherical particles at 40% wt. doping. This composition exhibited the highest ionic conductivity of 4.44×10^{-5} S cm^{-1}, attributed to enhanced ionic mobility facilitated by increased amorphous content. When employed in DSSC fabrication, the 40% wt. *o*-phenylenediamine–doped PVDF/LiI/I_2 electrolyte yielded the highest power conversion efficiency (PCE) of 3.1% under standard illumination (AM 1.5G, 100 mW cm^{-2}). These findings underscore the effectiveness of molecular doping strategies in tuning polymer electrolyte properties and highlight the potential of *o*-phenylenediamine modified PVDF systems for next-generation DSSCs. In addition, the developed polymer electrolyte system demonstrates potential for integration into flexible, low-cost, solar-driven power modules for adaptive portable assistive power devices.

1. Introduction

Advanced solar cell technologies have emerged in response to the pressing global need for renewable and sustainable energy sources. A lot of research has been done on alternative energy technologies because of the increasing demand for clean, renewable energy around the world. One of the most promising of these technologies is still solar energy. Over the past few decades, dye-sensitized solar cells (DSSCs) have attracted a lot of interest as an affordable and sustainable substitute for photovoltaic technology [1]. DSSCs have recently become a viable alternative in energy generation because of its affordability, effectiveness, and limitless potential. A promising type of third-generation solar cells, DSSCs are characterized by their low cost of production, relatively simple architecture, environmental friendliness, and good performance in diffuse and low-intensity light [2–5]. Another benefit of the variety of organic molecules that may be used to build DSSCs is that they allow for the creation of different donors, acceptors, and interfaces.

DSSC consist of four components, a mesoporous nanocrystalline

* Corresponding authors.
E-mail addresses: kotties555@gmail.com (S. Kotteswaran), rbalubio@gmail.com (R. Balu).

https://doi.org/10.1016/j.mseb.2025.118907
Received 11 May 2025; Received in revised form 9 October 2025; Accepted 16 October 2025

semiconductor (typically TiO_2), a photosensitizing dye, a redox electrolyte (commonly I^-/I_3^-), and a counter electrode [6]. Enhancing every component of DSSCs is necessary to raise their overall efficiency. The ability to be produced in various colours, potential, high transparency and high efficiency particularly in ambient light conditions along with low energy production and the use of sustainable and non-toxic materials are some of the distinctive aspects of DSSCs [7]. As the light-harvesting element, the sensitizing dye is essential to the design of DSSC. DSSCs exploit three primary classes of dyes—Ruthenium (II) polypyridyl complexes, porphyrin-based sensitizers and metal-free D–π–A organic dyes. Ru-based dyes (e.g., N749, C101, N719) achieve maximum PCE with improved ligands and cyclometallation strategies aimed at broad absorption and stabilized excited states [8]. Due to their superior light absorption over the visible spectrum and effective injection into the semiconductor, the use of ruthenium-based dyes, such as N_3 and its variants, contributed to the initial achievements of DSSCs [9]. However, Ruthenium dyes were retard by their high cost and lack of environmental qualities, despite their great stability and efficiency. Because of these shortcomings, organic dyes have emerged as a possible remedy. Novel organic dyes with broad absorption bands and adaptable molecular architectures based on donor-π-acceptor complexes may be an affordable, high-performing material of choice [10].

The stability and overall conversion efficiency of DSSCs are influenced by the electrolyte components. The electrolyte must possess both significant ionic conductivity and thermal stability. Because it improves charge transmission between the photoanode and cathode. Perfect electrolyte solvent has low viscosity, low vapor pressure, high boiling point, and exceptional dielectric characteristics, natural degeneracy, resilience and ease of preparation [11]. Three different categories of electrolytes are available for DSSCs: liquid, solid state and quasi solid state [12]. Electrolytes are often liquid in nature; however, they can also be quite corrosive, volatile and dry out with time, which reduces the device's functionality. The liquid electrolyte that has been employed in DSSCs has a number of disadvantages the solid-state electrolytes have been created to increase performance and stability in order to address such maintenance issues [13]. The solid electrolyte differs from all other electrolytes in that it is leakage-free. Polymer electrolytes offer more benefits and less disadvantages when compared to liquid electrolytes [14,15]. For DSSC applications, a variety of polymers have been employed as electrolytes, including polyethylene oxide (PEO) [16], poly (vinylidene fluoride-co-hexafluoropropylene) (PVDF-HFP) [17], poly vinylidene fluoride (PVDF) [18], poly (methyl methacrylate) (PMMA) [19], polyethylene glycol (PEG) [20,21], and polyacrylonitrile (PAN) [22]. PVDF was selected as the solid polymer electrolyte for the current study because of its strong electron-withdrawing functional group (-C-F), high dielectric constant ($\varepsilon = 8.4$), and good mechanical strength. Furthermore, PVDF exhibits stability against a wide range of organic compounds and corrosive substances, such as halogens, alkalis, and acids. Because of its small ionic radius and strong electronegativity, the fluorine atom in -C-F has the best ionic transport and lowers the rate of recombination at the semiconductor/polymer electrolyte interface in DSSCs [23].

When nitrogen-containing organic compounds were added as a dopant to solid polymer electrolyte-based DSSCs, it was found that the interaction between I^-/I_3^- redox couple and the lone pair of electrons in the nitrogen atom of the amine group increased the short circuit current (I_{sc}) and open circuit voltage (V_{oc}) [24]. Better miscibility, increased conductivity, and improved DSSC performance are actually demonstrated by the PVDF polymer electrolyte. Adding dopants to polymer electrolytes is used to reduce crystallinity and improve electrical conductivities. The advantage of this latter approach that the organic nitrogenous compounds in the polymer electrolyte contribute a lone pair of electrons that work with the iodine in the redox couple to reduce iodine sublimation, which improves the conductivities of the polymers and the DSSC's performance [25].

The introduction of organic nitrogenous substances into the electrolyte tends to boost the V_{oc} and move the negative band of TiO_2 [26]. When the electrical performance of diphenylamine (DPA) and phenothiazine (PT) in DSSC was compared, it was found that the phenothiazine doped polymer blend electrolyte had an increased conductivity. Under 70 mW cm^{-2} of illumination, the DSSC produced employing the PT doped polymer electrolyte good power conversion efficiency (η) [27]. The aforementioned findings show that, in comparison to the DPA doped PVDF/KI/I_2 polymer blend electrolyte, the electron density of PT appears to lead to a considerably stronger interaction with iodine in the redox pair. In order to create a unique doped multi-polymer blend electrolyte system solvent-free for dye-sensitized solar cell (DSSC) applications, an organic nitrogenous molecule must be doped. Specifically, coupled with KI and I_2, this new electrolyte is mixed with poly (vinylidene fluoride) (PVDF) and added to the produced 2,6-bis (2-thio pyridyl) pyridine (BTPP). Under simulated sunlight radiation of 80 mW/cm^2, the current–voltage (I–V) characteristics of the nanocrystalline DSSC fabricated using the present electrolyte yield considerable energy conversion efficiency [28]. In comparison to polymers containing 2,5-pyridine, 2,6−/3,5-pyridine, 3,5-pyridine units showed the highest levels of electrochemical behaviour. It seems that, the presence of electron-withdrawing pyridine unit, which has N in its structure, these polymers' lower reduction potential suggested that they had good electron-transporting and facile electron-injection capabilities. The above studies shows that the organic compound containing Nitrogen decrease the crystallinity, increase the conductivity and electrochemical stability [29].

In this present research work used a solution casting approach with DMF as the solvent to make O-Phenylenediamine doped PVDF/LiI/I_2 electrolyte films at varying weight percentages (0%, 10%, 20%, 30%, 40%, 50%). In order to optimize the optimal polymer electrolyte composition, the effects of different concentration of O-Phenylenediamine with respect to LiI doped polymer electrolyte, the structural, morphological and electrochemical properties of the PVDF/LiI/I_2 electrolyte have been studied. Ultimately, a DSSC has been constructed with the improved polymer electrolyte, and its photovoltaic characteristics have also been examined.

2. Experimental section

2.1. Materials

Sigma Aldrich provided commercially obtainable polymer PVDF (MW ~ 2,75,000 g/mol), O-Phenylenediamine, Fluorine-doped tin oxide (FTO) glass plate, Tritonx100, Chloroplatinic acid hydrate, Titanium Tetrachloride, Titanium Dioxide, 4-tert-butanol. We bought Lithium iodide (LiI), *N*, *N*-dimethyl formamide (DMF), iodine (I_2) in SDFCL, India. Acetone, Isopropyl alcohol, Acetyl acetone, Ethanol, Acetonitrile, Butanol was purchased from Sisco Research Laboratories private limited, India. Titanium diisopropoxide bis(acetylacetonate), N719 Dye, Iodolyte, Teflon tape was purchased from Solaronix`, SA. For all the compounds, no further purification was needed.

2.2. Preparation of polymer electrolyte film

Polymer electrolyte fibres were made via the solution casting technique [30]. In 20 ml of DMF, 0.3 g of PVDF, 0.03 g of LiI, and 0.006 g of I_2 were first dissolved. By adding various weight percentages (0%, 10%,20%, 30%, 40% and 50% with regard to LiI) of O-Phenylenediamine to the aforementioned polymer solution, distinct weight percentages (wt%) of O-Phenylenediamine doped solid polymer electrolytes were formed.

An electromagnetic stirrer was used to agitate the mixture at 80^0C until a homogenous polymer electrolytic solution was achieved. The prepared solution was poured in the glass petri dish. After that, to eliminate the solvent, petri dish filled with the homogeneous electrolytic solution was kept in a vacuum oven for 12 h at 60 °C for drying. The

polymer electrolyte sheets were formed with different weight percentage of O-Phenylenediamine with respect to Lithium Iodide. The polymer electrolyte was taken for further characterizations once the solvent has evaporated. Schematic diagram of Synthesis of polymer electrolyte was shown in the Fig. 1.

2.3. Characterization of polymer electrolyte film

Following characterization techniques were used to study the polymer electrolyte film. With the use of Cu-Kα radiation and a Bruker-advance D8 X-ray diffraction meter, the XRD patterns of the as-prepared O-Phenylenediamine doped PVDF / LiI / I_2 polymer electrolyte sheets were captured. Using an electrochemical workstation (model CH-608E) from CH Instrument Inc., USA, the impedance spectra of the polymer electrolyte sheets were measured by means of the AC-impedance technique at room temperature (303*K*). The frequency range covered by the workstation was 20 Hz to 1 MHz. The impedance spectra were used to calculate the bulk resistance of the polymer electrolyte. Using a stainless-steel electrode that contained polymer electrolyte, the ionic conductivity of the polymer electrolyte was determined.

2.4. Fabrication of dye sensitized solar cell

The third part of the DSSC is the redox electrolyte, which is placed between the working and counter electrodes. Fluorine-doped with tin oxide (FTO) glasses are first cleaned for 30 min in an ultrasonic bath using distilled water, ethanol, and acetone. TiO_2 colloidal paste was created by combining 0.5 g of TiO_2 with Triton X 100 and acetylacetone using a doctor blade technique, and it was then applied to the FTO electrode. The TiO_2 mesoporous layer was 12 μm thick, and the light-scattering layer was 5 μm, giving a total thickness of 17 μm and a metal mask with 0.16 cm^2 aperture was used during photovoltaic measurements under 100 mW/cm^2 illumination to minimize light scattering and ensure measurement accuracy. The device's active area was 0.25 cm^2. The FTO glass plate was calcined at 450 °C. After being treated with $TiCl_4$, the TiO_2-coated film was sintered at 450 °C for 30 min. Then 0.5×10^{-3} M of N719 (photo sensitizer) containing 4-tertiary butanol and acetonitrile in a 1:1 volume ratio was then used to submerge the TiO_2-coated electrode for a whole day. The TiO_2 electrode connected to the N719 was washed with 100% ethanol and left to dry in a N_2 flow for 30 min in order to remove the unabsorbable dye. Eventually, the dye-coated adsorbed photoanode was created. The FTO glass plate was coated with chloroplatinic acid to form the photocathode as a Pt-counter electrode, and it was subsequently dried at 450 °C. Fig. 2 depicted the electron transport mechanism of the DSSC.

When incident light (photon) is absorbed by a photo sensitizer, the dyes electrons transition from their ground state (s) to their excited state (S*). The electrode's nanopore TiO_2 conduction band, which lies underneath the dye excited state and is where a very small percentage of UV sun photons are absorbed by the material, is now filled with excited electrons with a nanosecond lifetime. These injected electrons diffuse in the direction of the back contact as they move between TiO_2 nanoparticles. Through the external circuit, electrons reach the area around the counter electrode. I_3^- is reduced to I^- by the counter electrode's electrons. This leads to dye regeneration and oxidation of I^- to I_3^- (oxidized state). The acceptance of the electrons from the I^- ion redox mediator results in the dye ground states regeneration. Once more, as the mediator (I_3^-) diffuses in the direction of the counter electrode, it transforms into an I^- ion.

3. Results and discussion

3.1. Powder X-ray diffraction (PXRD) analysis

The purpose of the XRD investigation was to look into the composition of the polymer electrolytic fibres [31]. The XRD patterns of pure and various weight percentages of O-Phenylenediamine doped PVDF / LiI / I_2 electrolytes are shown in Fig. 3 (a-f). On the other hand, the undoped PVDF/ LiI / I_2 electrolytes, the XRD peaks are observed with

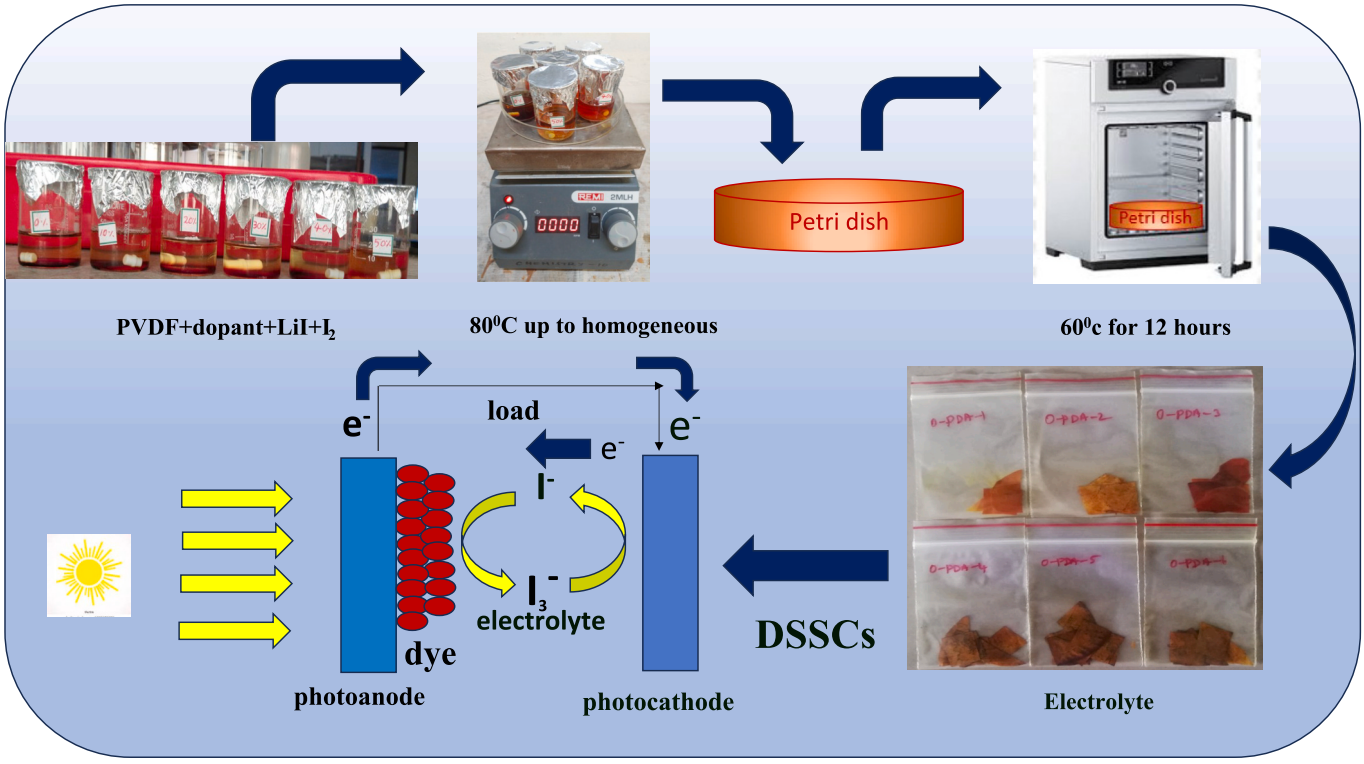

Fig. 1. Graphical representation of synthesis of O-Phenylenediamine doped PVDF / LiI / I_2 electrolytic films.

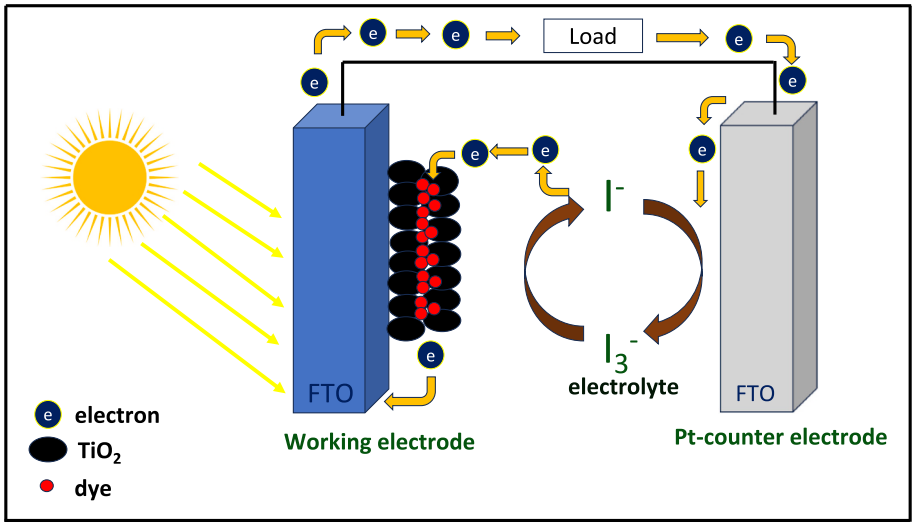

Fig. 2. Schematic illustration of the electron transport mechanism of Dye Sensitized Solar Cell.

TiO_2/N_3–Dye/PVDF/LiI/I_2/Graphite (i)

TiO_2/N_3–Dye/40%O – Phenylenediamine doped PVDF/LiI/I_2/Graphite (ii)

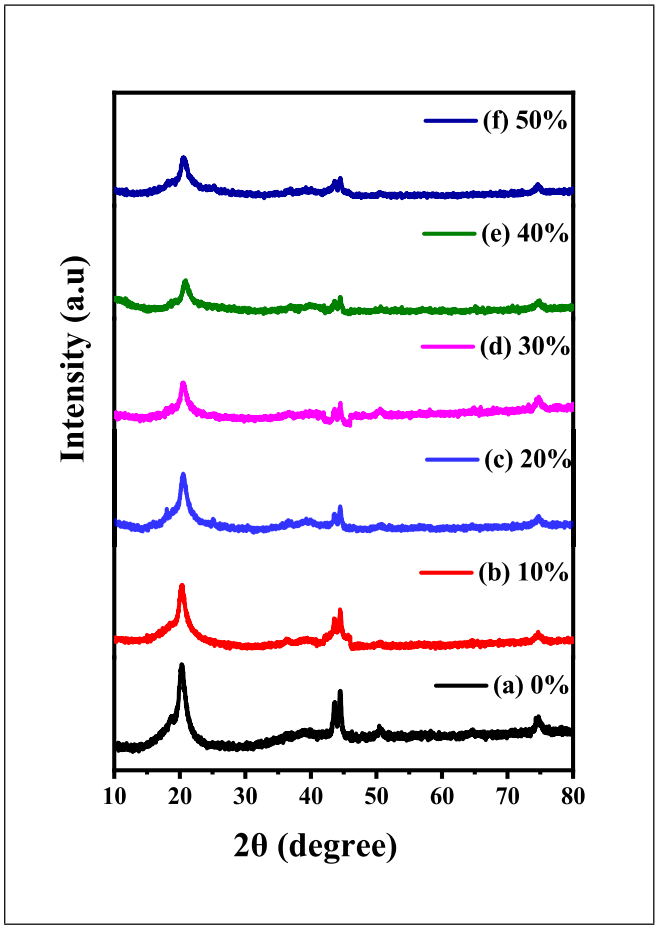

Fig. 3. (a-f): PXRD patterns of O-Phenylenediamine (a) 0%, (b) 10%, (c) 20%, (d) 30%, (e) 40% and (f) 50% doped PVDF/ LiI / I_2 electrolytic films.

typical scanning angles of $2\theta = 20.36°$, 25.18°, and 35.94°. The peak in regard to the strength has been gradually reduced by up to 40% with the addition of *O*-phenylenediamine. It was discovered that these diffraction peaks' intensity was lower than that of the pure polymer [32]. This shown that *O*-phenylenediamine (0%, 10%, 20%, 30%, and 40%, 50%) doped PVDF/ LiI / I_2 electrolyte films had reduced crystallinity. The tendency that has been observed may be explained by the fact that *O*-phenylenediamine doped PVDF/ LiI / I_2 electrolytes are more amorphous than pure undoped PVDF / LiI / I_2.

The peak intensity steadily rises after 40%. The polymer chain rearrangement is hampered when O-Phenylenediamine is introduced to pure PVDF/ LiI / I_2, leading to a noticeably disordered polymer structure. Nevertheless, it was shown that these peak intensities dropped as O-Phenylenediamine was added up to 40 wt%. This outcome verified the higher crystallinity of the PVDF/ LiI / I_2 electrolyte film doped with 50% O-Phenylenediamine. The data led us to conclude that the electrolyte film with the lowest crystallinity is the PVDF/ LiI / I_2 polymer doped with 40% *o*-phenylenediamine and it has more amorphous than the other electrolytes, which enhanced the polymer's ionic conductivity.

3.2. AC-impedance analysis

The ionic conductance of the polymer electrolyte doped with *O*-phenylenediamine was ascertained using the electrochemical impedance plots [33]. Fig. 4 (a-f) displays the AC-impedance spectra of PVDF/ LiI / I_2 with O-Phenylenediamine with various composition. The effect of blocking electrodes is responsible for the low-frequency range's linear region and the high-frequency region in the semicircle, which is caused by the bulk effect of the electrolyte. Based on the AC-impedance spectrum [34], the ionic conductivity (σ) of the polymer electrolyte layer was determined using the formula.

Ionic conductivity $(\sigma) = t/R_b{}^*A$.

Thickness of the polymer electrolyte is denoted by **'t'.**

The polymer electrolyte layer covers the electrode area is denoted by **'A'.**

Polymer blend electrolyte's bulk resistance is denoted by **'R_b'.**

When the concentration of the dopant is paired with improved charge carrier ion concentration along with ionic mobility, magnitude of

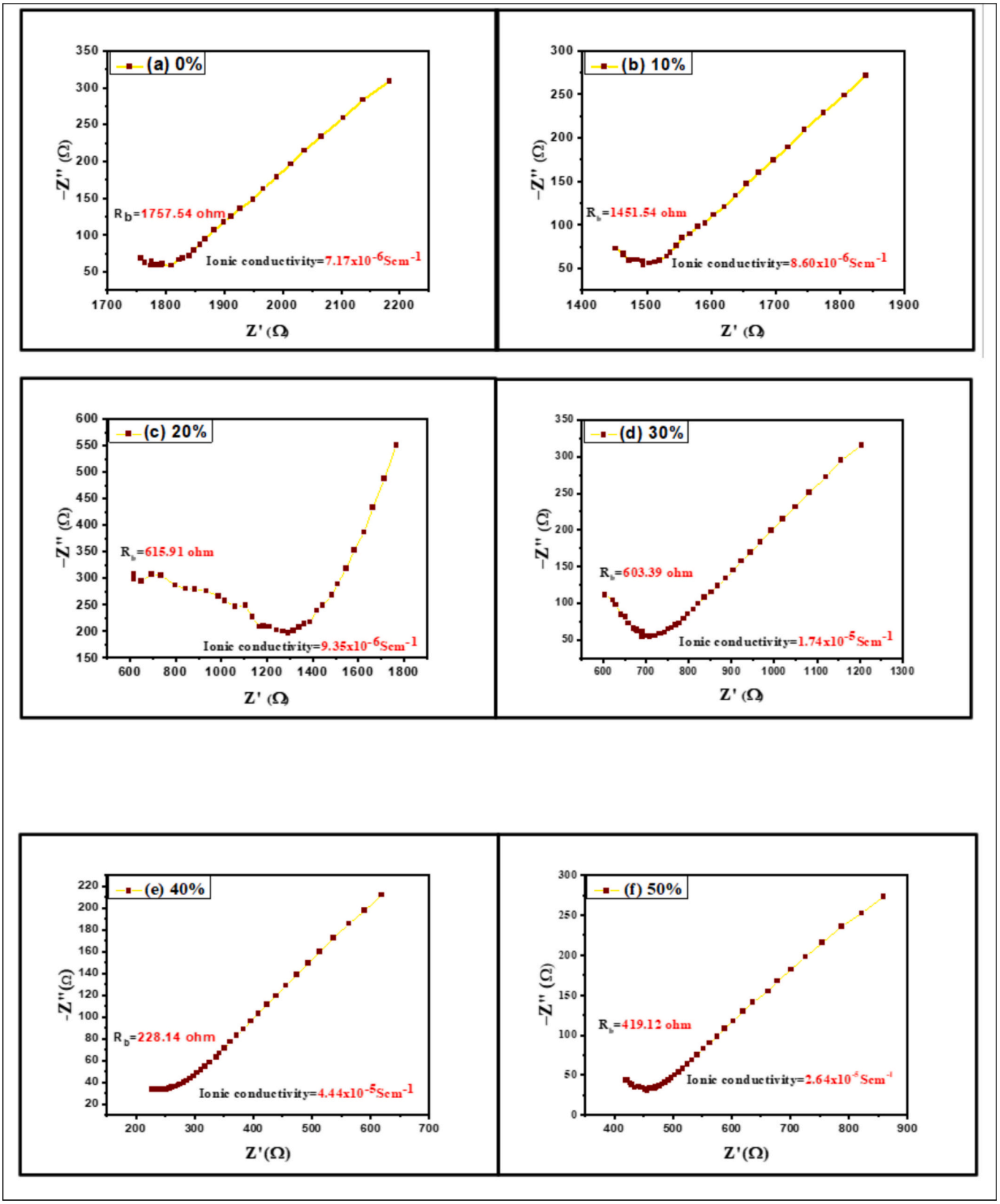

Fig. 4. (a-f): AC-Impedance Analysis of O-Phenylenediamine (a) 0%, (b) 10%, (c) 20%, (d) 30%, (e) 40% and (f) 50% doped PVDF/ LiI / I_2 electrolytic films.

the resistance of the polymer electrolyte system decreases [35]. The ionic conductance of undoped PVDF/ LiI / I_2 is 7.17 × 10–6 Scm^{-1}. After the addition of O-Phenylenediamine in PVDF/ LiI / I_2, there was an increase in ionic conductivity as 8.60 × 10^{-6} Scm^{-1} for the weight percentage of 10, 9.35 × 10^{-6} Scm^{-1} for 20 wt%, 1.74 × 10^{-5} Scm^{-1} for 30 wt%, for 40 wt% the ionic conductivity was 4.44 × 10^{-5} Scm^{-1}. This was listed in Table 1. The greatest value of ionic conductivity is reached at 40% weight percentage of *O*-phenylenediamine-doped PVDF/ LiI / I_2.

This tendency may be due to the inclusion of the organic substance *O*-phenylenediamine, which contains nitrogen, to the PVDF/ LiI / I_2 polymer electrolyte. O-Phenylenediamine and iodine form a charge-transfer complex that lowers iodine sublimation, improving conductivity and photon-to-current conversion efficiency. PVDF/ LiI / I_2 containing 50 wt% of O-Phenylenediamine shows the reduced ionic conductivity value as 2.6 × 10^{-5} Scm^{-1}. The quick increase in viscosity inflicts the ionic conduction channels by absorbing some free space, which restricts the charge carriers' mobility, may be the causes of this pattern. The addition of 40% O-Phenylenediamine resulted in the highest ionic conductivity value, which may be related to the polymer electrolyte's enhanced chain mobility as well as the inhibition of PVDF/ LiI / I_2 crystal formation. Therefore, the comprehensive photon-to-current transformation ability is determined by the movement of the redox pair as well as the ionic conductivity behaviour of polymer electrolytes [36].

The equivalent circuit of the solid polymer electrolyte consist of resistance of the electrolyte (R_S) in Ohms which related to electrolyte bulk resistance, the charge transfer resistance (*R*ct) in Ohms related to the electron transfer at the interface, a constant phase element (CPE) in $S.s^{-n}$, n is the exponent of CPE and the Warburg impedance (W) in Ohms represent diffusion controlled impedance were shown in Fig. 5, and the value of individual components are calculated are shown in Table 2. All the electrochemical impedance plots are showing same pattern of electronic circuit.

Among the individual values of electrical components of impedance, the Warburg impedance arises due to the diffusion of electrolyte. It represents the resistance to mass transport ion diffusion within the electrolyte. A high Warburg impedance means that ions are having difficulty diffusing through the material leads to poor ionic transport. A low Warburg impedance implies that ions can diffuse more easily indicates good ionic transport, which directly implies higher ionic conductivity. 40% doped polymer electrolyte shows low Warburg impedance; hence it has higher ionic conductivity comparing with all other percentages of *o*-phenylenediamine doped solid polymer electrolyte.

3.3. Morphological studies

Scanning electron microscopic (SEM) technique [37] is used to investigate the surface morphology of *O*-phenylenediamine doped with PVDF/ LiI / I_2 polymer electrolyte. Fig. 6 (a-f) displays the pictures of PVDF/ LiI / I_2 polymer electrolyte doped with O-Phenylenediamine obtained in the SEM technique.

Comparing the 0% O-Phenylenediamine doped with PVDF/ LiI / I_2 SPE to 10%, 20%, 30%, 40%, and 50% O-Phenylenediamine doped with PVDF/ LiI / I_2 polymer electrolyte, Large, spherical particles with spaces are shown in the 0% SPE's SEM image. The addition of O-Phenylenediamine dopant causes a progressive 40% reduction in the size of spherical particles. Beyond 40%, the spherical particles size rises. The tiny spherical particles present along with the presence of vacancies are the factors which cause the ionic conductance of the PVDF/ LiI / I_2 polymer electrolyte and photocathode of the DSSC.

Table 1
Ionic Conductivity of dye – sensitized solar cell (DSSC)s of O-Phenylenediamine doped with (a) 0%, (b) 10%, (c) 20%, (d) 30%, (e) 40% and (f) 50% PVDF/ LiI / I_2 electrolytes.

Electrolyte	O-Phenylenediamine (%)	Ionic Conductivity ($S.cm^{-1}$)
a	0	7.17 × 10^{-6}
b	10	8.60 × 10^{-6}
c	20	9.35 × 10^{-6}
d	30	1.74 × 10^{-5}
e	40	4.44 × 10^{-5}
f	50	2.64× 10^{-5}

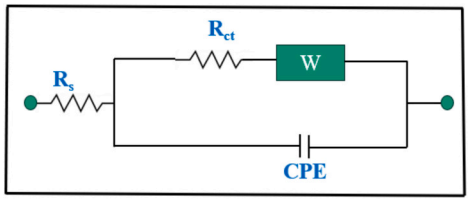

Fig. 5. Equivalent circuit impedance model for solid polymer electrolytes.

Table 2
Different Values of Electrical Components of different weight percentages of *o*-phenylenediamine doped PVDF/LiI/I_2 polymer electrolyte.

% of *o*-phenylene diamine doped-PVDF/LiI/I_2.	R_s Ohms	R_{ct} Ohms	CPE S. s^{-n}	n	W Ohms
0%	1750	1810	5 × 10^{-3}	0.8	50
10%	1410	1500	3 × 10^{-6}	0.8	50
20%	610	1210	5 × 10^{-6}	0.8	150
30%	550	700	5 × 10^{-4}	0.8	60
40%	230	250	5 × 10^{-2}	0.8	30
50%	410	450	6 × 10^{-2}	0.8	35

3.4. Photovoltaic measurements of dye sensitized solar cells

The dye – sensitized solar cell (DSSC)s was built using O-Phenylenediamine (0%, 10%, 20%, 30%, 40%, and 50%) doped PVDF/ LiI / I_2 electrolytes. Fig. 7 (a-f) displays the current density-voltage (I-V) curves of dye – sensitized solar cell (DSSC)s with *O*-phenylenediamine doped with PVDF/ LiI / I_2 electrolytes (0%, 10%, 20%, 30%, 40%, and 50%).

O-Phenylenediamine doped with different weight percentage (0%, 10%, 20%, 30%, 40%, and 50%) of PVDF/ LiI / I_2 electrolytes reveal the following photo voltaic parameters: J_{sc} = 5.93 mA/cm^2, V_{oc} = 0.75 V, FF = 0.30 and η = 1.3%; J_{sc} = 6.45 mA/cm^2, V_{oc} = 0.75 V, FF = 0.33 and η = 1.6%; J_{sc} = 7.61 mA/cm^2, V_{oc} = 0.76 V, FF = 0.32 and η = 1.8%; J_{sc} = 9.58 mA/cm^2, V_{oc} = 0.76 V, FF = 0.33 and η = 2.4%; J_{sc} = 11.9 mA/cm^2, V_{oc} = 0.75 V, FF = 0.36 and η = 3.1% and J_{sc} = 8.45 mA/cm^2, V_{oc} = 0.75 V, FF = 0.32 and η = 2.0%, independently.

The following formula is used to determine the dye-sensitized solar cell's (DSSC) efficiency:

$$\eta\ (\%) = (V_{oc}\ x\ I_{sc}\ x\ FF/P_{in})\ x\ 100.$$

where 'FF' represents the fill factor, 'η' for power transformation efficiency, 'V_{oc}' for open circuit voltage, 'I_{sc}' for short circuit current density and 'P_{in}' for incident light power [38].

These findings demonstrate that the performance of DSSCs using 40% doped *O*-phenylenediamine PVDF/ LiI / I_2 electrolyte is superior to that of DSSCs using 0%, 10%, 20%, 30%, or 50% doped O-Phenylenediamine PVDF/ LiI / I_2 electrolyte. This is because O-Phenylenediamine has the potential to donate electrons. Its structure contains atoms of nitrogen. It prevents I_2 from sublimating by generating a charge transfer complex with I_2 of I_3^-. I_3^-concentration is decreased by *O*-phenylenediamine, whereas I^- concentration is increased. The reaction

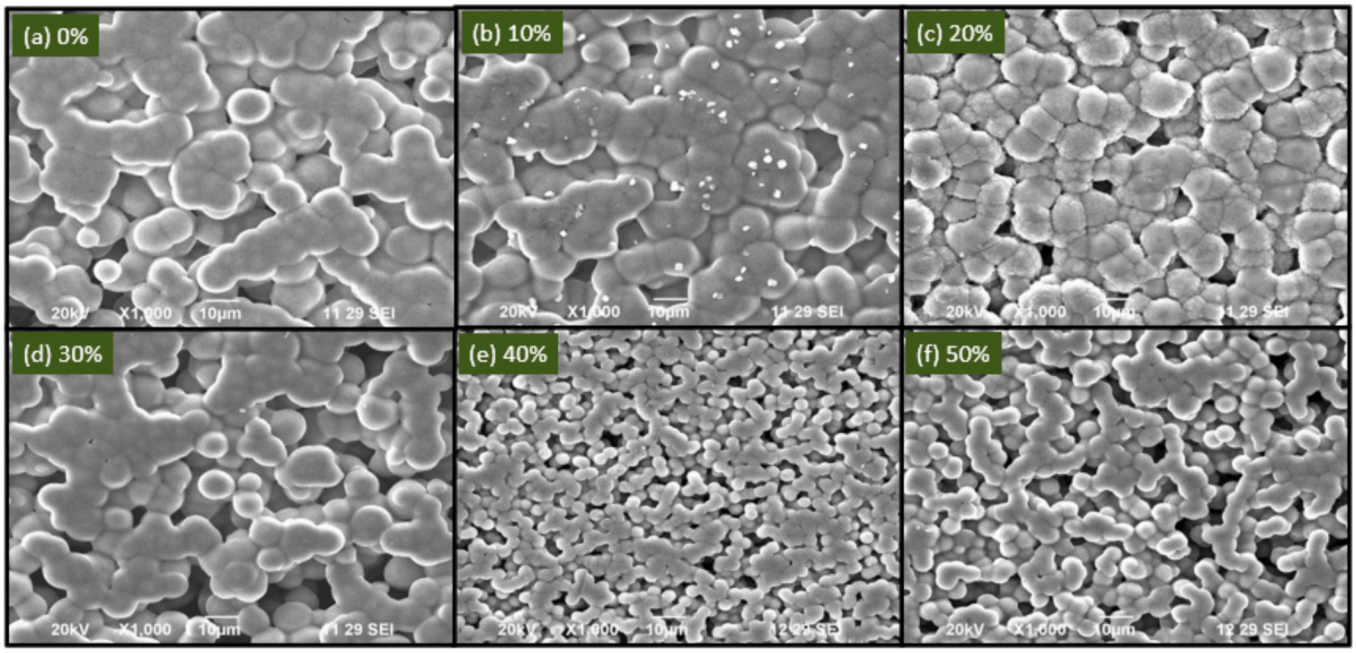

Fig. 6. (a-f): SEM images of O-Phenylenediamine (a) 0%, (b) 10%, (c) 20%, (d) 30%, (e) 40% and (f) 50% doped PVDF/ LiI / I_2 electrolyte films.

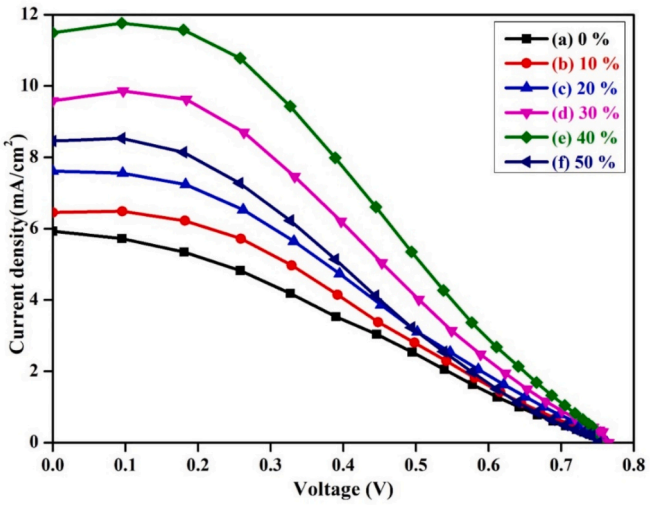

Fig. 7. (a-f): The photovoltaic (J-V) curves of dye – sensitized solar cell (DSSC)s with (a) 0%, (b) 10%, (c) 20%, (d) 30%, (e) 40% and (f) 50% O-Phenylenediamine doped with PVDF/ LiI / I_2 electrolytes.

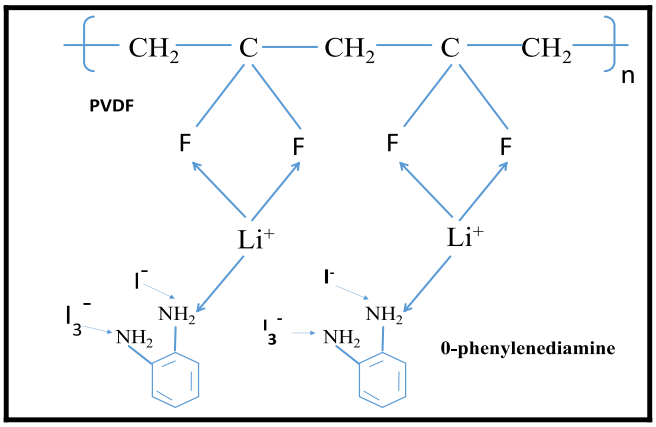

Fig. 8. Molecular interaction of O-Phenylenediamine with PVDF/ LiI / I_2.

between I_3^- at the TiO_2 semiconductor electrolyte junction and the injected electron reduces as a result of a drop in I_3^-concentration, which raises the electron concentration [39].

Fig. 8 depicts the interaction of O-Phenylenediamine with PVDF/ LiI / I_2. The DSSC with 40% *O*-phenylenediamine-doped PVDF/ LiI / I_2 electrolyte is the system with the elevated power transformation efficiency. The elevation of power transformation ability may be due to the fact that 40% O-Phenylenediamine doped PVDF/ LiI / I_2 electrolyte which has the best ionic conductivity and the lowest crystallinity. Table 3 shows the comparative study of the present work with the previous power conversion efficiency of DSSC.

Table 3
Solar cell efficiency comparison.

S. No	Doped Polymer Electrolyte	η (%)	Year	Reference
1	Phenothiazine- doped PVDF-HFP/KI/I_2	2.92%	2017	[40]
2	4-nitroaniline-doped PVDF-HFP/LiI/I_2	1.5%	2017	[41]
3	2-Amino-4,6-Dimethoxypyrimidine-doped PVDF/KI/I_2	2.5%	2020	[42]
4	40% O-Phenylenediamine-doped PVDF/ LiI/I_2	3.1%	2025	Present work

4. Conclusion

In conclusion, the solvent casting approach was used to prepare the various weight percentages of O-Phenylenediamine doped PVDF/ LiI / I_2 polymer electrolyte, including 0%, 10%, 20%, 30%, 40%, and 50%. The PVDF/ LiI / I_2 polymer electrolyte doped with 40% O-Phenylenediamine exhibits the lowest crystallinity. The 40% O-Phenylenediamine doped PVDF/ LiI / I_2 polymer electrolyte has the smallest spherical, void-filled particles as their surface morphology. The PVDF/ LiI / I_2 polymer electrolyte doped with 40% O-Phenylenediamine has the excessive ionic conductance value, measuring 4.44 × 10^{-5} Scm^{-1}. With a 3.1% photocathode value, 40% O-Phenylenediamine doped with PVDF/ LiI / I_2 polymer electrolyte-based dye – sensitized solar cell (DSSC) has the

maximum performance. This is due to the polymer electrolyte's maximum ionic conductivity and lowest crystallinity.

CRediT authorship contribution statement

K. Sathya: Writing – original draft, Formal analysis, Data curation, Conceptualization. **D. Janet:** Formal analysis, Data curation, Conceptualization. **S. Kannadhasan:** Resources, Formal analysis, Data curation, Conceptualization. **P. Sudhakar:** Formal analysis, Data curation, Conceptualization. **S. Kotteswaran:** Writing – review & editing, Supervision, Investigation, Formal analysis, Data curation, Conceptualization. **Saravanan Pandiaraj:** Funding acquisition, Formal analysis, Data curation, Conceptualization. **G Ahilandeswari:** Funding acquisition, Formal analysis, Data curation, Conceptualization. **Gautham Devendrapandi:** Formal analysis, Data curation, Conceptualization. **Ranjith Balu:** Writing – review & editing, Supervision, Formal analysis, Data curation, Conceptualization.

Ethical approval

Not required.

Funding source

No funding for this research.

Declaration of competing interest

The authors declare that they have no known competing financial interests or personal relationships that could have appeared to influence the work reported in this paper.

Acknowledgments

The authors extend their appreciation to the King Salman center for Disability Research for funding this work through Research Group No. KSRG-2024-394.

Research data policy and data availability statements

The authors declare that the data supporting the findings of this study are available within the paper.

Declarations

Consent to participate: The authors agreed that they participating in the research work.

Consent to publish: The authors agreed to publish this research paper.

Data availability

Data will be made available on request.

References

[1] Edson Evangelista, Iva S. de Jesus, Fernanda P. Pauli, Acácio S. de Souza, A. Amanda de, Maria Vitória Borges, S.F. Gomes, Vitor F. Ferreira, C. Fernando de, Mauricio A. da Silva, Melo, and Luana da SM Forezi., Recent advances in the application of Coumarins as photosensitizers for the construction of a dye-sensitized solar cell, ACS omega 10 (14) (2025) 13726–13748.

[2] Anik Sen, Miftahussurur Hamidi Putra, Abul Kalam Biswas, Anil Kumar Behera, Axel Groβ, Insight on the choice of sensitizers/dyes for dye sensitized solar cells: a review, Dyes Pigments 213 (2023) 111087.

[3] Youn Soo Masud, Kim, and Hwan Kyu Kim., Quasi-solid-state dye-sensitized solar cells by mechanically stable semi-interpenetrating network polymer gel electrolytes for indoor applications, ACS Appl Energy Mater 7 (12) (2024) 5226–5234.

[4] Haoran Zhou, Md Aftabuzzaman, Sung Ho Kang Masud, Hwan Kyu Kim, Key materials and fabrication strategies for high-performance dye-sensitized solar cells: comprehensive comparison and perspective, ACS Energy Lett. 10 (2) (2025) 881–895.

[5] Ben Xiang, Wei-Li An, Fu Ji-Jiang, Shi-Xiong Mei, Si-Guang Guo, Xu-Ming Zhang, Biao Gao, Paul K. Chu, Graphene-encapsulated blackberry-like porous silicon nanospheres prepared by modest magnesiothermic reduction for high-performance lithium-ion battery anode, Rare Metals 40 (2) (2021) 383–392.

[6] Aswani Yella, Hsuan-Wei Lee, Hoi Nok Tsao, Chenyi Yi, Aravind Kumar Chandiran, Md Khaja Nazeeruddin, Eric Wei-Guang Diau, Chen-Yu Yeh, Shaik M. Zakeeruddin, Michael Grätzel, Porphyrin-sensitized solar cells with cobalt (II/III)–based redox electrolyte exceed 12 percent efficiency, science 334 (6056) (2011) 629–634.

[7] Simon Mathew, Aswani Yella, Peng Gao, Robin Humphry-Baker, Basile F. E. Curchod, Negar Ashari-Astani, Ivano Tavernelli, Md Ursula Rothlisberger, Khaja Nazeeruddin, Michael Grätzel, Dye-sensitized solar cells with 13% efficiency achieved through the molecular engineering of porphyrin sensitizers, Nat. Chem. 6 (3) (2014) 242–247.

[8] Daniela F.S.L. Rodrigues, Carlos M.R. Abreu, Frédéric Sauvage, Jorge F.J. Coelho, Arménio C. Serra, Dzmitry Ivanou, Adélio Mendes, Improved interfacial electron dynamics with block poly (4-vinylpyridine)–poly (styrene) polymers for efficient and long-lasting dye-sensitized solar cells, ACS Applied Polymer Materials 6 (15) (2024) 8939–8949.

[9] Daniela Sayah, Tarek H. Ghaddar, Investigation of Ethylisopropyl sulfone medium with a copper-based redox electrolyte for ambient light dye-sensitized solar cells: achieving high efficiency and enduring long-term stability, ACS Appl Energy Mater 6 (23) (2023) 11924–11933.

[10] Vasan Iyer, Jan Petersen, Sebastian Geier, Peter Wierach, Development and multifunctional characterization of a structural sodium-ion battery using a high-tensile-strength poly (ethylene oxide)-based matrix composite, ACS Appl Energy Mater 7 (9) (2024) 3968–3982.

[11] Hwan Kyu Kim, Advanced polymeric matrices for gel electrolytes in quasi-solid-state dye-sensitized solar cells: Recent progress and future perspective, Materials Today Energy 38 (2023) 101440.

[12] Mingwei Zhao, Shichun Liu, Caili Dai, Ruoqin Yan, Yang Li, Peng Liu, Development and drag reduction behaviors of a water-in-water emulsion polymer drag reducer, ACS Applied Polymer Materials 5 (5) (2023) 3707–3716.

[13] David Müller, Ershuai Jiang, Paula Rivas-Lazaro, Clemens Baretzky, Georgios Loukeris, Shankar Bogati, Stefan Paetel, et al., Indoor photovoltaics for the internet-of-things–a comparison of state-of-the-art devices from different photovoltaic technologies, ACS Appl Energy Mater 6 (20) (2023) 10404–10414.

[14] Shanmuganathan Venkatesan, I-Ting Chuang, Hsisheng Teng, Yuh-Lang Lee, High-performance carbon black-based counter electrodes for copper (I)/(II)-mediated dye-sensitized solar cells, ACS Sustain. Chem. Eng. 11 (32) (2023) 12166–12176.

[15] Kyeong Min Kim, Hwan Kyu Kim, Highly efficient gel electrolytes by end group modified PEG-based ABA triblock copolymers for quasi-solid-state dye-sensitized solar cells, Chem. Eng. J. 420 (2021) 129899.

[16] Caihong Wang, Xueyong Li, Jiwen Zhou, Wen Tian, Junyi Ji, Wu Yong, Shuai Tan, Poly (ionic liquid) bridge joining smectic lamellar conducting channels in photoelectrochemical devices as high-performance solid-state electrolytes, ACS Appl Energy Mater 4 (9) (2021) 9479–9486.

[17] Masud, Hwan Kyu Kim, Redox shuttle-based electrolytes for dye-sensitized solar cells: comprehensive guidance, recent progress, and future perspective, ACS Omega 8 (7) (2023) 6139–6163.

[18] Evan, Md Sadik Hussain, et al., "polyethylene oxide-based nanocomposites as polymer electrolytes for dye-sensitized solar cell application." ECS journal of solid-state, Sci. Technol. 12 (11) (2023) 115004.

[19] Zakaria, P. N. M., Saaid, F. I., Raffi, A. A. M., Noor, I. S. M., Woo, H. J., & Tan, W. (2023, March). Efficiency enhancement of dye-sensitized solar cell with PVdF-HFP: MPII: NaI quasi-solid-state electrolyte. In IOP Conference Series: Earth and Environmental Science (Vol. 1151, No. 1, p. 012053). IOP Publishing.

[20] Mi-Ra Kim, et al., Investigation of the photovoltaic effect in dye-sensitized solar cells based on poly (ethylene glycol) -nanofiber electrolytes, Bull Korean Chem Soc 44 (12) (2023) 1008–1014.

[21] A. Manap, S. Mahalingam, R. Rabeya, K.S. Lau, C.H. Chia, P.J. Liew, Effect of polyethylene glycol in graphene quantum dots for dye-sensitized solar cell, Polym. Bull. (2024) 1–12.

[22] Herlin Pujiarti, Zahrotul Ayu Pangestu, Nabella Sholeha, Nasikhudin Nasikhudin, Markus Diantoro, Joko Utomo, Muhammad Safwan Abd Aziz, The effect of acetylene carbon black (ACB) loaded on Polyacrylonitrile (PAN) nanofiber membrane electrolyte for DSSC applications, Micromachines 14 (2) (2023) 394.

[23] Sandhia Bai, A. Amirruddin, A. Pandey, M. Samykano, Muhammad Ahmad, Kamal Sharma, V.V. Tyagi, Advancements in the development of various types of dye-sensitized solar cells: a comparative review, Energy Engineering: Journal of the Association of Energy Engineers 118 (4) (2021) 737.

[24] S. Kamesh, et al., Nitrogen-doped reduced graphene oxide enfolded zinc cobaltite micro flowers as efficient triiodide reduction for a platinum-free counter electrode in dye-sensitized solar cell applications, Electrochim. Acta 475 (2024) 143262.

[25] R.N. Iman, M. Younas, K. Harrabi, A. Mekki, A comprehensive review on advancements and optimization strategies in dye-sensitized solar cells: Components, characterization, stability and efficiency enhancement, Inorg. Chem. Commun. 112488 (2024).

[26] Henok Tibebu Weldemicheal, Mekonnen Abebayehu Desta, Yedilfana Setarge Mekonnen, Derivatized photosensitizer for an improved performance of the dye-sensitized solar cell, Results in Chemistry 5 (2023) 100838.

[27] S. Ganesan, B. Vinod Mathew, Joseph Paul, P. Maruthamuthu, S. Austin Suthanthiraraj, Influence of organic nitrogenous compounds phenothiazine

and diphenyl amine in poly (vinylidene fluoride) blended with poly (ethylene oxide) polymer electrolyte in dye-sensitized solar cells, Electrochim. Acta 102 (2013) 219–224.
[28] S. Ganesan, P. Karthika, R. Rajarathinam, M. Arthanareeswari, Vinod Mathew, P. Maruthamuthu, A poly (ethylene oxide), poly (vinylidene fluoride) and polycapro lactone polymer blend doped with an indigenous nitrogen–sulfur based organic compound as a novel electrolyte system for dye-sensitized solar cell applications, Sol. Energy 135 (2016) 84–91.
[29] Santhosh Kamaraj, Ganesan Shanmugam, Ahalya Gunasekeran, Balamurugan Selvaraj, Eswaramoorthi Thirugnanasambandam, Mohanraj Kandhasamy, Anandan Sambandam, Performance of 4-Subsituted pyridine based additive and cobalt redox in poly (ethylene glycol)–Hydroxyethylcellulose polymer electrolytes with DTTCY acid sensitizer on dye sensitized solar cells, Energy Fuel 35 (18) (2021) 15045–15057.
[30] S. Chowdhury, Kuaanan Techato, N719 dye as a sensitizer for dye-sensitized solar cells (DSSCs): a review of its functions and certain rudimentary principles, Environ. Prog. Sustain. Energy 42 (1) (2023) e13955.
[31] Phuti S. Ramaripa, et al., Influence of phthalocyanine nanowire dye on the performance of titanium dioxide-metal organic framework nanocomposite for dye-sensitized solar cells, Chemical Engineering Journal Advances 14 (2023) 100485.
[32] R.N. Iman, M. Younas, K. Harrabi, A. Mekki, A comprehensive review on advancements and optimization strategies in dye-sensitized solar cells: components, characterization, stability and efficiency enhancement, Inorg. Chem. Commun. 165 (2024) 112488.
[33] Zakaria PN, Saaid FI, Raffi AA, Noor IS, Woo HJ, Tan W. Efficiency enhancement of dye-sensitized solar cell with PVdF-HFP: MPII: NaI quasi-solid-state electrolyte. InIOP conference series: earth and environmental science 2023 mar 1 (Vol. 1151, no. 1, p. 012053). IOP Publishing.
[34] Kannadhasan Sundaramoorthy, Senthil Pandian Muthu, Ramasamy Perumalsamy, Effects of 2-Amino-4, 6-Dimethoxypyrimidine on PVDF/KI/I 2-based solid polymer electrolytes for dye-sensitized solar cell application, J. Electron. Mater. 49 (2020) 3728–3734.
[35] A. Subramanian, S. Murugapoopathi, K.T. Amesho, Enhancing the performance of Nanocrystalline TiO2 dye-sensitized solar cells with phenothiazine-doped blended solid polymer electrolyte, Electrocatalysis 15 (2) (2024) 226–238.
[36] Mohammad Bagher Karimi, et al., A comprehensive review on the proton conductivity of proton exchange membranes (PEMs) under anhydrous conditions: proton conductivity upper bound, Int. J. Hydrog. Energy 46 (69) (2021) 34413–34437.
[37] Mohd Saiful Asmal Rani, et al., The development of poly (ethylene oxide) reinforced with a nanocellulose-based nanocomposite polymer electrolyte in dye-sensitized solar cells, Materials Advances 2 (16) (2021) 5465–5470.
[38] Haoran Zhou, Jung-Min Ji, Hyun Seok Lee, Mohammad Aftabuzzaman Masud, Dong-Nam Lee, Chul Hoon Kim, Hwan Kyu Kim, D-π-a structured porphyrin and organic dyes with easily synthesizable donor units for low-cost and efficient dye-sensitized solar cells, ACS Appl. Mater. Interfaces 15 (33) (2023) 39426–39434.
[39] Ji, Jung-Min, Haoran Zhou, Yu Kyung Eom, Chul Hoon Kim, and Hwan Kyu Kim. "Dye-sensitized solar cells: 14.2% efficiency dye-sensitized solar cells by co-sensitizing novel thieno [3, 2-b] indole-based organic dyes with a promising porphyrin sensitizer (Adv. Energy Mater. 15/2020)." Adv. Energy Mater. 10, no. 15 (2020).
[40] D. Devadiga, M. Selvakumar, D. Devadiga, T.N. Ahipa, P. Shetty, S. Paramasivam, S.S. Kumar, Synthesis and characterization of a new phenothiazine-based sensitizer/co-sensitizer for efficient dye-sensitized solar cell performance using a gel polymer electrolyte and Ni–TiO 2 as a photoanode, New J. Chem. 46 (44) (2022) 21373–21385.
[41] S. Kannadhasan, M. S. Pandian & P. Ramasamy, Synthesis of pure and 4-Nitroaniline doped (PVDF-HFP/LiI/I2) polymer electrolyte for dye sensitized solar cell (DSSC) applications. In AIP Conference Proceedings, AIP Publishing, (Vol. 1832, No. 1). (2017, May).
[42] Kannadhasan Sundaramoorthy, Senthil Pandian Muthu, Ramasamy Perumalsamy, Effects of 2-Amino-4, 6-Dimethoxypyrimidine on PVDF/KI/I 2-based solid polymer electrolytes for dye-sensitized solar cell application, J. Electron. Mater. 49 (2020) 3728–3734.